

Association Between SARS-CoV-2 Infection and Immune-Mediated Myopathy in Patients Who Have Died

Tom Aschman, MD; Julia Schneider, MSc; Selina Greuel, MD; Jenny Meinhardt, MD; Simon Streit, MD; Hans-Hilmar Goebel, MD; Ivana Büttnerova, MD; Sefer Elezkurtaj, MD; Franziska Scheibe, MD; Josefine Radke, MD; Christian Meisel, MD; Christian Drosten, MD; Helena Radbruch, MD; Frank L. Heppner, MD; Victor Max Corman, MD; Werner Stenzel, MD

 Supplemental content

IMPORTANCE Myalgia, increased levels of creatine kinase, and persistent muscle weakness have been reported in patients with COVID-19.

OBJECTIVE To study skeletal muscle and myocardial inflammation in patients with COVID-19 who had died.

DESIGN, SETTING, AND PARTICIPANTS This case-control autopsy series was conducted in a university hospital as a multidisciplinary postmortem investigation. Patients with COVID-19 or other critical illnesses who had died between March 2020 and February 2021 and on whom an autopsy was performed were included. Individuals for whom informed consent to autopsy was available and the postmortem interval was less than 6 days were randomly selected. Individuals who were infected with SARS-CoV-2 per polymerase chain reaction test results and had clinical features suggestive of COVID-19 were compared with individuals with negative SARS-CoV-2 polymerase chain reaction test results and an absence of clinical features suggestive of COVID-19.

MAIN OUTCOMES AND MEASURES Inflammation of skeletal muscle tissue was assessed by quantification of immune cell infiltrates, expression of major histocompatibility complex (MHC) class I and class II antigens on the sarcolemma, and a blinded evaluation on a visual analog scale ranging from absence of pathology to the most pronounced pathology. Inflammation of cardiac muscles was assessed by quantification of immune cell infiltrates.

RESULTS Forty-three patients with COVID-19 (median [interquartile range] age, 72 [16] years; 31 men [72%]) and 11 patients with diseases other than COVID-19 (median [interquartile range] age, 71 [5] years; 7 men [64%]) were included. Skeletal muscle samples from the patients who died with COVID-19 showed a higher overall pathology score (mean [SD], 3.4 [1.8] vs 1.5 [1.0]; 95% CI, 0-3; $P < .001$) and a higher inflammation score (mean [SD], 3.5 [2.1] vs 1.0 [0.6]; 95% CI, 0-4; $P < .001$). Relevant expression of MHC class I antigens on the sarcolemma was present in 23 of 42 specimens from patients with COVID-19 (55%) and upregulation of MHC class II antigens in 7 of 42 specimens from patients with COVID-19 (17%), but neither were found in any of the controls. Increased numbers of natural killer cells (median [interquartile range], 8 [8] vs 3 [4] cells per 10 high-power fields; 95% CI, 1-10 cells per 10 high-power fields; $P < .001$) were found. Skeletal muscles showed more inflammatory features than cardiac muscles, and inflammation was most pronounced in patients with COVID-19 with chronic courses. In some muscle specimens, SARS-CoV-2 RNA was detected by reverse transcription-polymerase chain reaction, but no evidence for a direct viral infection of myofibers was found by immunohistochemistry and electron microscopy.

CONCLUSIONS AND RELEVANCE In this case-control study of patients who had died with and without COVID-19, most individuals with severe COVID-19 showed signs of myositis ranging from mild to severe. Inflammation of skeletal muscles was associated with the duration of illness and was more pronounced than cardiac inflammation. Detection of viral load was low or negative in most skeletal and cardiac muscles and probably attributable to circulating viral RNA rather than genuine infection of myocytes. This suggests that SARS-CoV-2 may be associated with a postinfectious, immune-mediated myopathy.

Author Affiliations: Author affiliations are listed at the end of this article.

Corresponding Authors: Tom Aschman, MD (tom.aschman@charite.de), and Werner Stenzel, MD (werner.stenzel@charite.de), Department of Neuropathology, Charité-Universitätsmedizin Berlin, corporate member of Freie Universität Berlin and Humboldt-Universität zu Berlin, Charitéplatz 1, 10117 Berlin, Germany.

JAMA Neurol. 2021;78(8):948-960. doi:10.1001/jamaneurol.2021.2004
Published online June 11, 2021. Corrected on August 12, 2021.

In 2019, a new coronavirus variant with drastic global impact emerged; it currently sums up to 168 million confirmed cases of severe acute respiratory syndrome coronavirus 2 (SARS-CoV-2) infection and an estimated 3.5 million deaths from coronavirus disease 2019 (COVID-19).¹ Independent studies suggest that 30% to 60% of patients with SARS-CoV-2 infections experience myalgia.²⁻⁴ Myalgia and increased levels of creatine kinase were found to be more pronounced in patients with critical illness needing intensive care support than individuals who were mildly affected.⁵⁻⁷ Signs of skeletal muscle injury were associated with a more severe clinical course and higher mortality rates.^{7,8} Several case reports describe rhabdomyolysis,⁹⁻¹⁴ and magnetic resonance imaging findings have suggested myositis.¹⁵⁻¹⁸ To our knowledge, 3 case reports included biopsies, 2 of which advocated a dermatomyositis-like phenotype.¹⁸⁻²¹ Finally, in a large follow-up study, two-thirds of survivors of COVID-19 experienced fatigue or muscle weakness and 2% to 3% myalgia, even 6 months after an infection with SARS-CoV-2.²² Similar results have been found elsewhere.^{23,24}

Myopathy ranging from mild myositis to fatal rhabdomyolysis has been associated with many different viruses.²⁵⁻³⁹ However, muscle biopsies are rarely performed in clinically suspected cases of virus-associated myositis. Therefore, until now, to our knowledge, only case reports and small series offer some histopathological insights. Here, we report comprehensive histopathological, virological, immunological, and ultrastructural findings of skeletal muscle samples from individuals who died with severe COVID-19 in comparison with patients with critical illnesses that were not COVID-19.

Methods

Study Design

Between March 2020 and February 2021, cryopreserved tissue samples of quadriceps and deltoid muscles and cryopreserved or formalin-fixed paraffin-embedded samples of lung and heart tissue samples were obtained from individuals who died with clinical features of COVID-19 (atypical, bilateral pneumonia in chest computed tomography and characteristic laboratory findings). Exclusion criteria were a postmortem interval of more than 6 days and lack of cryopreserved skeletal muscle specimens. In addition, cryopreserved deltoid and/or quadriceps muscle tissues and formalin-fixed paraffin-embedded-preserved heart and lung samples from individuals with nasopharyngeal swabs negative for SARS-CoV-2 and absence of clinical features of COVID-19 infection were used as controls; these were individuals with critical illness who had nonseptic or septic clinical courses and underwent routine autopsy (Table; eTable 1 in the Supplement). Clinical records were consulted for age, sex, preexisting medical conditions, onset of clinical symptoms, length of hospitalization, duration of intensive care treatment, laboratory results, therapeutic measures, and complications. In all individuals, a whole-body autopsy was performed at the Departments of Pathology and Neuropathology, Charité-Universitätsmedizin Berlin, Berlin, Germany. The primary cause of death was defined

Key Points

Question Is there a COVID-19-associated myopathy, and is it a viral or postviral phenomenon?

Findings In this case-control autopsy study, 26 of 43 individuals (60%) who had died with a diagnosis of COVID-19 showed signs of muscle inflammation, ranging from mild to severe inflammatory myopathy. Inflammation was more pronounced in patients who were chronically ill and those who had seroconverted to SARS-CoV-2 than those who died after acute or subacute courses of COVID-19 and those who died of other illnesses, and no evidence was found for a direct infection of muscle tissue.

Meaning In this study, SARS-CoV-2 was associated with an immune-mediated myopathy.

as the condition or injury that initiated the sequence of events leading to death.⁴⁰

This study was approved by the local ethics committees as well as by the Charité-Berlin Institute of Health COVID-19 research board and was in compliance with the Declaration of Helsinki; autopsies were performed on the legal basis of section 1 of the Autopsy Act of the State of Berlin and section 25(4) of the German Infection Protection Act. Informed consent to autopsy was either given by patients themselves, close relatives, or their legal guardians. Strengthening the Reporting of Observational Studies in Epidemiology (STROBE) reporting guidelines were followed.

Virological and Serological Testing

Unfixed and cryopreserved or native tissue samples were used for detection and quantification of SARS-CoV-2 RNA by quantitative reverse transcription-polymerase chain reaction (RT-qPCR) in skeletal muscle, heart, and lung samples, as described previously.^{41,42} Only samples with at least 2 positive results were considered positive. Oligonucleotides targeting the leader transcriptional regulatory sequence and a region within the single-guide RNA encoding the SARS-CoV-2 *E* gene were used to detect single-guide RNA, as described previously.^{42,43}

We performed anti-SARS-CoV-2 IgG enzyme-linked immunosorbent assays in serum samples using a commercially available kit (Anti-SARS-IgG Kit [Euroimmun]), with an optical density ratio of 1.1 as the threshold for positivity. Antinuclear antibody assays, myositis-specific autoantibodies (antinuclear matrix protein-2 [anti-NXP2], anti-transcriptional intermediary factor 1γ [anti-TIF1γ], anti-melanoma differentiation-associated gene 5 [anti-MDA5], anti-signal recognition particle [anti-SRP], anti-Mi2, anti-isoleucyl-transfer RNA [tRNA] synthetase [anti-OJ], anti-glycyl-tRNA synthetase [anti-EJ], anti-threonyl-tRNA synthetase [anti-PL7], anti-alanyl-tRNA synthetase [anti-PL12], antihistidyl tRNA synthetase [anti-Jo1], and anti-small ubiquitin-like modifier-1 activating enzyme [anti-SAE]), and myositis-associated autoantibodies (anti-Ku, anti-PM75, anti-PM100, and anti-Ro52) were conducted in serum samples according to the manufacturer's instructions (ANA-Mosaik 1A EuroPattern and EuroLine,

Table. Patient Characteristics^{a,b}

Characteristic	Patients, No. (%)				
	With COVID-19				Without COVID-19
	Total	Acute	Subacute	Chronic	
Patient characteristics					
Total	43	13	16	14	11
Age, median (IQR), y	72 (16)	79 (12)	69 (18)	70 (9)	71 (5)
<35	4 (9)	0	2 (13)	2 (14)	0
35-59	3 (7)	0	2 (13)	1 (7)	0
60-69	10 (23)	2 (16)	4 (25)	4 (29)	5 (45)
70-79	17 (40)	5 (38)	5 (31)	7 (50)	6 (55)
>80	9 (21)	6 (46)	3 (19)	0	0
Sex					
Female	12 (28)	3 (23)	7 (44)	2 (14)	4 (36)
Male	31 (72)	10 (77)	9 (56)	12 (85)	7 (64)
BMI					
Patients with data, No.	42	8	15	14	11
Median (IQR)	28.5 (8)	25.5 (8)	28.0 (13)	30.5 (6)	33.7 (11)
Postmortem interval, median (IQR), h ^c	45 (38)	44 (23)	48 (51)	45 (21)	42 (70)
Duration of illness, median (IQR), d ^d	24 (23)	10 (6)	24 (9)	51 (35)	21 (12)
Days in hospital, median (IQR) [No. of patients with data]	20 (25) [42]	7 (9) [12]	18 (9) [16]	43 (34) [14]	17 (14) [11]
Days in intensive care unit, No. (%) [No. of patients with data]	15 (26) [42]	4 (5) [12]	15 (9) [16]	40 (20) [14]	8 (12) [11]
Complications					
Acute respiratory distress syndrome	37 (86)	10 (77)	14 (88)	13 (93)	4 (36)
Acute kidney failure	31 (72)	7 (54)	11 (69)	13 (93)	9 (82)
Acute liver failure	14 (33)	3 (23)	5 (31)	6 (43)	4 (36)
Bacterial pneumonia	22 (51)	4 (31)	9 (56)	9 (64)	6 (55)
Sepsis or septic shock	24 (56)	2 (15)	10 (63)	12 (86)	7 (64)
Treatments, No. (%)					
Invasive ventilation	28 (65)	3 (23)	11 (67)	14 (100)	9 (82)
Kidney replacement therapy	21 (49)	3 (23)	8 (50)	10 (71)	9 (82)
Extracorporeal membrane oxygenation	16 (37)	1 (8)	5 (31)	10 (71)	3 (27)
Catecholamines	29 (67)	3 (23)	12 (75)	14 (100)	9 (82)
Corticosteroids, No. (%) [No. of patients with data]	20 (49) [41]	6 (46) [11]	10 (63) [16]	4 (29) [14]	1 (9) [11]
Intravenous immunoglobulin, No. (%) [No. of patients with data]	3 (7) [41]	0 [11]	0 [16]	3 (22) [14]	1 (9) [11]
No. (%) [No. of patients with data]	2 (5) [41]	0 [11]	1 (6) [16]	1 (7) [14]	1 (9) [11]
Laboratory values^{a,b,e}					
Creatine kinase values, U/L					
First, median (IQR) [No. of patients with data]	206 (365) [38]	153 (382) [8]	233 (376) [16]	210.5 (262) [14]	97 (103) [10]
Last, median (IQR) [No. of patients with data]	164 (392) [38]	315 (273) [8]	171 (609) [16]	58 (206) [14]	175 (567) [10]
Highest, median (IQR) [No. of patients with data]	600 (748) [38]	359 (583) [9]	694 (706) [16]	808 (1374) [14]	485 (885) [11]
Creatine kinase-MB fraction values, U/L					
First, median (IQR) [No. of patients with data]	23 (24) [31]	18 (32) [6]	22 (6) [15]	32 (25) [13]	36 (23) [9]
Last, median (IQR) [No. of patients with data]	24 (26) [31]	29 (24) [6]	26 (25) [15]	17.7 (27) [13]	35 (50) [9]
Highest, median (IQR) [No. of patients with data]	41 (29) [39]	35 (73) [7]	41 (20) [15]	42 (23) [14]	55 (269) [10]

(continued)

Table. Patient Characteristics^{a,b} (continued)

Characteristic	Patients, No. (%)				Without COVID-19
	Total	Acute	Subacute	Chronic	
Troponin values, ng/mL					
First, median (IQR) [No. of patients with data]	0.040 (0.070) [30]	0.074 (0.149) [8]	0.043 (0.044) [11]	0.035 (0.068) [11]	0.065 (0.105) [10]
Last, median (IQR) [No. of patients with data]	0.069 (0.149) [30]	0.108 (0.832) [8]	0.052 (0.054) [11]	0.106 (0.116) [11]	0.113 (0.236) [10]
Highest, median (IQR) [No. of patients with data]	0.103 (0.152) [32]	0.127 (0.920) [8]	0.078 (0.063) [12]	0.138 (0.107) [12]	0.118 (0.257) [10]
Ferritin values, ng/mL					
First, median (IQR) [No. of patients with data]	1377 (2083) [36]	1418 (3011) [8]	1161 (549) [14]	1998 (3120) [14]	ND
Last, median (IQR) [No. of patients with data]	2779 (7537) [36]	1843 (8080) [8]	2048 (3272) [14]	6436 (12 422) [14]	ND
Highest, median (IQR) [No. of patients with data]	3995 (10 691) [36]	1852 (7845) [8]	2466 (3656) [14]	10 958 (36 849) [14]	ND
Interleukin 6 values, pg/L					
First, median (IQR) [No. of patients with data]	152 (570) [30]	146 (9443) [5]	174 (567) [13]	139 (357) [12]	ND
Last, median (IQR) [No. of patients with data]	282 (988) [30]	362 (9534) [5]	282 (993) [13]	424 (778) [12]	ND
Highest, median (IQR) [No. of patients with data]	926 (5926) [33]	362 (3745) [7]	892 (2998) [14]	1894 (8377) [13]	ND
No. of positive SARS-CoV-2 polymerase chain reaction test results, median (IQR)	2 (5)	1 (1)	3 (3.5)	5 (5.5)	0 ^f

Abbreviations: BMI, body mass index (calculated as weight in kilograms divided by height in meters squared); IQR, interquartile range; ND, no data.

SI conversion factors: To convert creatine kinase to $\mu\text{kat/L}$, multiply by 0.0167; ferritin to $\mu\text{g/L}$, multiply by 1.0; troponin to $\mu\text{g/L}$, multiply by 1.0.

^a Numbers were rounded, and percentages may not add to 100 because of rounding.

^b In cases in which data were not available for all patients, numbers of patients with data are indicated.

^c Defined as the number of hours between time of death and start of autopsy.

^d Defined as the delay between the first symptoms that led to hospitalization and death.

^e First, last, and highest values available per patient and hospitalization. When only 1 value was available, this one was classified as the highest.

^f All control patients were tested at least once, with a median (interquartile range) of 2 (3) nasopharyngeal swabs per patient.

Autoimmune Inflammatory Myopathies 16 Ag immunoassay [Euroimmun]).

Histology and Immunohistochemistry

Specimens from quadriceps and deltoid muscles were snap frozen and stored at -80°C until further workup. Samples of lung and heart tissues were either fixed in formalin or cryopreserved. Stains on cryopreserved samples were performed on 7- μm cryomicrotome sections, and stains on formalin-fixed paraffin-embedded tissue were performed on 4- μm sections. Routine histological staining (hematoxylin-eosin, Gömöri trichrome, and periodic acid-Schiff) were performed according to standard procedures. Immunohistochemical staining was performed on a Benchmark XT autostainer (Ventana Medical Systems), as described previously.⁴⁴ Immunohistochemical de-

tection of SARS-CoV-2 was performed as described previously.⁴²

Semiquantitative Scores

Semiquantitative scores were generated for major histocompatibility complex class I (human leukocyte antigen [HLA]-ABC), class II (HLA-DR), CD45, CD68, CD8, and NKp46. Ten random fields of vision were viewed independently by 2 experienced morphologists (W.S. and T.A.) at $\times 400$ magnification with an Olympus BX50 microscope (Ocular WH10X-H/22; high-power field). Positive staining results with MHC class I (DAKO; clone W6/32, 1:100) and MHC class II (DAKO; MO775, 1:100) were defined as a clear upregulation on the sarcolemma; capillaries and arterioles were used as internal positive controls. For quantification of endomysial immune cell

populations, antibodies against CD45 (DAKO; clone UCHL1, 1:100), CD68 (DAKO; clone EBM11, 1:100), CD8 (DAKO; clone C8/144B, 1:100), and NKp46 (R&D Systems; clone MAB1850, 1:100) were used. Positively stained cells were counted and summed up for 10 high-power fields of vision.

Modified Visual Analog Scale Score

We defined 3 categories of muscle pathology (inflammation, necrosis, and degeneration) and applied a modified visual analog scale score inspired by Wedderburn et al.⁴⁵ The overall pathology score was the global visual analog scale score, taking into account all 3 categories. All specimens were viewed in a blinded manner and graded on a severity scale from 0 (no pathology) to 10 (most pronounced pathology) by 2 observers independently (W.S. and T.A.).

Electron Microscopy

Electron microscopy was performed on quadriceps muscle specimens from individuals with light microscopic signs of myositis, as described previously.⁴² At least 100 capillaries were assessed per sample, and images were interpreted by 2 neuropathologists (W.S. and H.H.G.) with long-standing experience in ultrastructural analysis.

Statistical Analysis

Statistical analyses were performed and graphs created with GraphPad Prism 9 (GraphPad Software). Heat map visualizations were created with Orange Data Mining software version 3.28.0 (University of Ljubljana)⁴⁶ and tables with Excel 2016 (Microsoft). Data are presented as counts and percentages, means (SDs), or medians (interquartile ranges [IQRs]). We performed normality testing in GraphPad Prism to decide on median vs mean data calculations. The Mann-Whitney *U* test was applied for comparison of 2 groups. No data points were excluded, and values were considered significant at $P < .05$.

Results

Patients Characteristics

Forty-three individuals with COVID-19 and 11 patients without COVID-19 were included. Of the 43 with COVID-19, 42 had a direct detection of SARS-CoV-2 RNA by nucleic acid amplification tests from the upper respiratory tract registered during the patient's life. In 1 case with clinical features suggestive of COVID-19 and serological proof of infection with SARS-CoV-2, no lifetime RT-qPCR data were available, but high viral loads were detected in the lower respiratory tract after death. In 3 individuals with COVID-19, only 1 of either quadriceps or deltoid muscle samples was collected. In the full cohort, detailed patient histories of 2 patients referred from other hospitals could not be retrieved; also, an insufficient quantity of tissue was preserved for analysis for 1 patient. The median age was 72 (IQR, 16; range, 26-92) years in the COVID-19 cohort and 71 (IQR, 5; range, 65-76) years in the control cohort. Most deceased individuals in both groups were men (31 of 43 with COVID-19 and 7 of 11 without COVID-19). The median duration of illness (DOI), defined as the number of days between the onset of symptoms that led to hos-

pitalization or the first positive RT-qPCR test results and the time of death, was 24 (range, 5-181) days in the COVID-19 cohort and 21 (range, 1-68) days in the control group. We determined 3 subgroups within the COVID-19 cohort: those with acute cases, with DOIs less than 15 days; subacute cases, with DOIs between 15 and 30 days; and chronic cases, with DOIs more than 30 days (Table).

All but 1 of the patients examined had concurrent medical conditions, but none was diagnosed with a primary myopathy during their lives. In 36 of 43 patients with COVID-19 (84%), COVID-19 was the primary underlying cause of death (eTable 1 in the Supplement).

All but 5 patients in the COVID-19 group (38 of 43) and all but 1 in the control cohort (10 of 11) were admitted to an intensive care unit. The median time in intensive care was 14.5 (range, 0-173) days in the COVID-19 and 8.0 (range, 0-43) days in the control group.

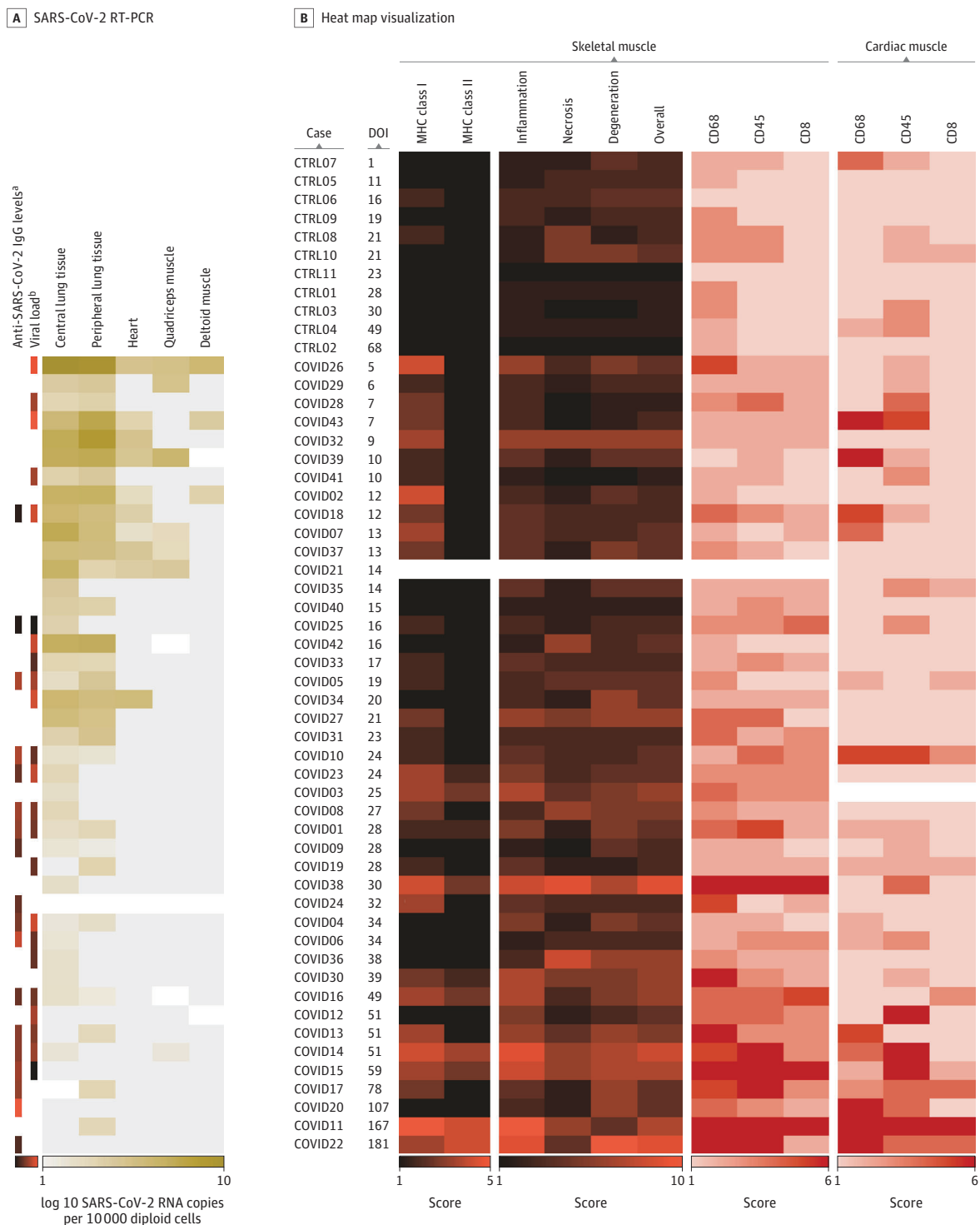
Detailed information on administered therapies was available for 41 patients with COVID-19. Twenty of these (49%) received corticosteroids, 3 (7%) received intravenous immunoglobulins, 2 (5%) received anakinra, and 1 (2%) received ruxolitinib. In the control group, 1 patient received intravenous immunoglobulins, dexamethasone, cyclophosphamide, and bortezomib as treatment for multiple myeloma.

The median of the first measured value of creatine kinase was significantly higher in the COVID-19 cohort (206 U/L [to convert to microkatal per liter, multiply by 0.0167]; range, 16-6367 U/L; 95% CI, 132-191 U/L; vs 97 U/L; range, 18-819 U/L; 95% CI, 18-254 U/L; $P = .045$). In total, 14 patients (33%) with COVID-19 and 2 control patients (18%) showed creatine kinase levels greater than 1000 U/L. Patients with chronic COVID-19 showed higher maximum ferritin levels (10 958 [95% CI, 3589-66 866] ng/mL) than patients with acute courses (1852 [95% CI, 102-50 974] ng/mL; $P = .04$) or subacute courses (2466 [95% CI, 1015-7674] ng/mL; $P = .004$) (Table). Procalcitonin, C-reactive protein, and leukocyte counts as nonspecific markers of systemic inflammation were comparable between groups (eTable 1 in the Supplement).

Virological Analysis

Testing for SARS-CoV-2 via RT-qPCR was positive in at least 1 of 2 different lung samples in 38 of 43 patients with COVID-19 (88%), heart tissue of 10 of 42 patients (23%), quadriceps muscle tissue of 7 of 41 patients (16%), and deltoid muscle tissue of 2 of 42 patients (5%). Subgenomic viral RNA was detected in samples from 20 patients (lung, 17; heart, 2; quadriceps muscle, 2; deltoid muscle, 1). Seroconversion had occurred in 17 of the 18 patients for which anti-SARS-CoV-2 antibodies were measured during their lives (Figure 1A). Viral load in lungs inversely correlated with the DOI (central lung specimens, log₁₀: Spearman r , -0.86 [95% CI, -0.93 to -0.75]; $P < .001$) and was higher in patients treated with corticosteroids (central lung specimens [log₁₀] of patients not treated with corticosteroids: $n = 20$; median [IQR], 2 [2.5] log₁₀ SARS-CoV-2 RNA copies per 10 000 diploid cells; vs those treated with corticosteroids: $n = 18$; median [IQR], 3 [4] log₁₀ SARS-CoV-2 RNA copies per 10 000 diploid cells; 95% CI, 1-6; $P < .01$) (Figure 1A; eFigure 3 in the Supplement).

Figure 1. Summary of Virological and Histopathological Findings



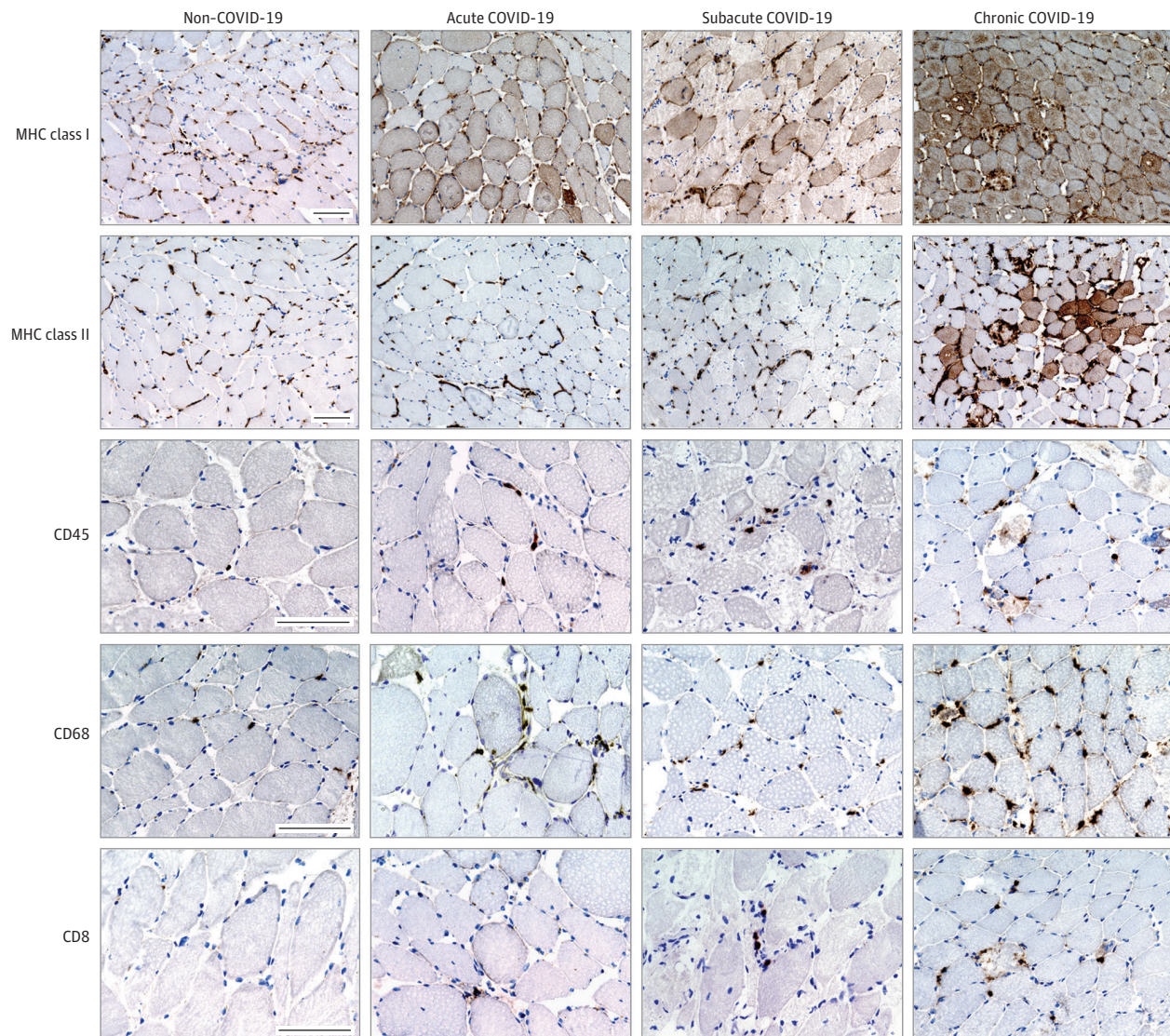
A, Quantification of SARS-CoV-2 RNA by reverse transcription–polymerase chain reaction (RT-PCR) tests of tissues in patients with COVID-19.

^a Serum anti-Sars-CoV-2 IgG levels (n = 17; black indicates a negative result; red, an optical density gradient).

^b Viral load from nasopharyngeal swabs within the 5 days prior to death by SARS-CoV-2 RNA RT-PCR testing (in copy numbers per microliter; n = 23; black indicates a negative result; red, a viral load gradient).

B, Heat map visualization of histopathological analysis of skeletal and heart muscle specimens. Scores are described in the methods section, absolute cell counts are shown in eTable 2 in the Supplement, and statistical analysis can be found in eFigure 2 in the Supplement. White rectangles indicate missing data. COVID followed by a number indicates a patient with COVID-19; CTRL followed by a number, a control patient; DOI, duration of illness; MHC, major histocompatibility complex.

Figure 2. Inflammatory Changes in Skeletal Muscles of Individuals Critically Ill With Diseases Other than COVID-19 Compared With Patients With COVID-19



Representative micrographs of postmortem samples from quadriceps muscles from a patient without COVID-19 (CTRL07), compared with samples from patients with acute (COVID37), subacute (COVID23), and chronic (COVID14)

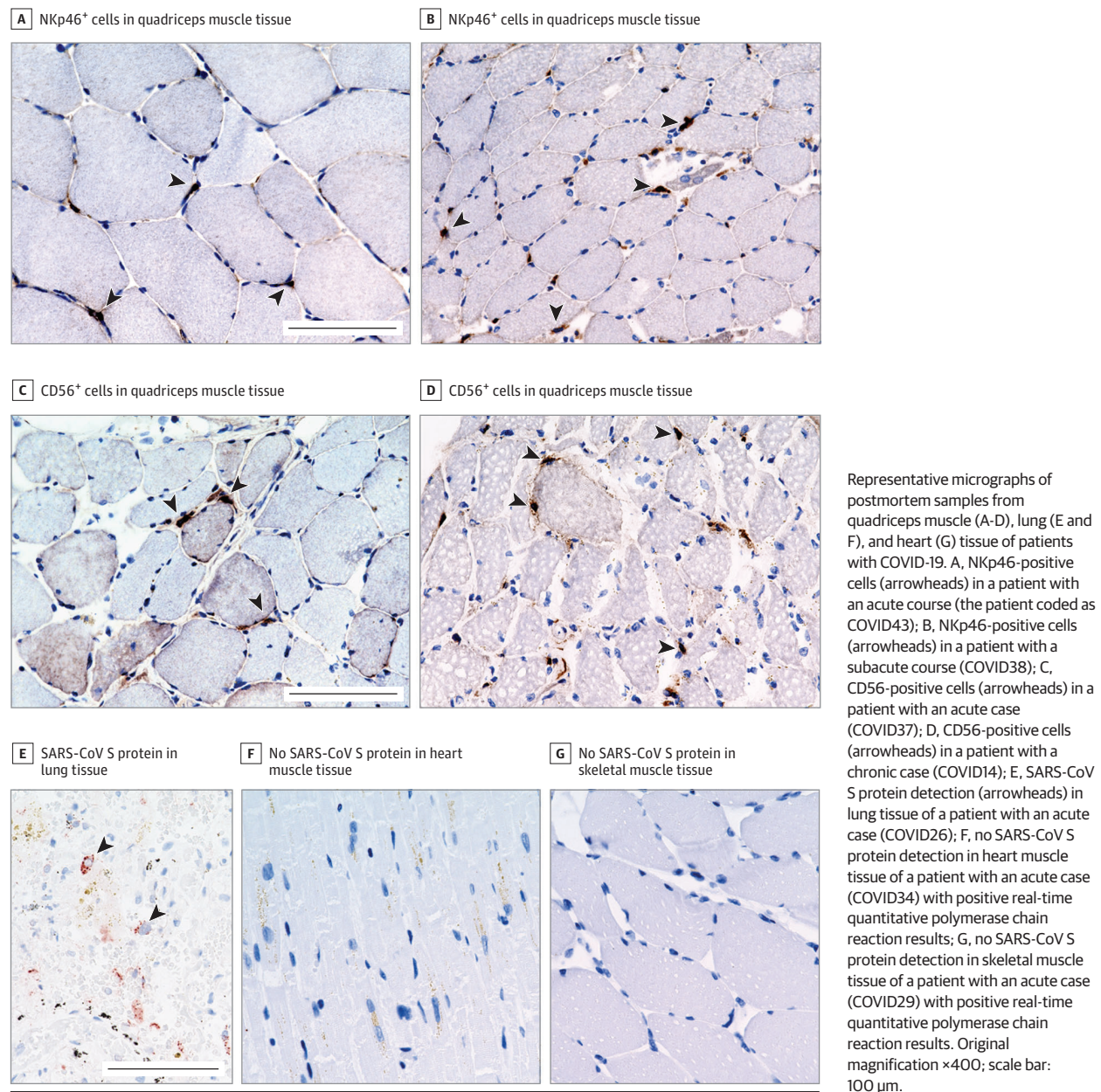
COVID-19 disease courses. Major histocompatibility complex (MHC) class I and MHC class II: original magnification $\times 200$; CD45, CD68, and CD8: original magnification $\times 400$; scale bars: 100 μm .

Histology and Immunohistochemistry of Skeletal Muscles

Patients with COVID-19 showed a higher mean (SD) overall pathology score (3.4 [1.8] vs 1.5 [1.0]; 95% CI, 0-3; $P < .001$). Among control patients, the highest score for inflammation was 2, while in the COVID-19 group, 26 of 42 cases (62%) showed a score higher than 2 (mean [SD], 3.5 [2.1] vs 1.0 [0.6]; 95% CI, 0-4; $P < .001$). Signs of degenerating muscle fibers were more frequently encountered in the COVID-19 cohort (mean [SD], 3.4 [1.8] vs 1.5 [1.4]; 95% CI, 0-4; $P < .005$). Clinically significant expression of MHC class I (HLA-ABC) antigens on the sarcolemma (defined as a score >1 of 6) could be found in 23 of 42 patients with COVID-19 (55%) but none of the controls. Upregulation of MHC class II (HLA-DR) was found in 7 of 42 patients with COVID-19

(17%), all of whom had a DOI longer than 21 days, and in none of the control samples (Figure 1; Figure 2; eTable 2 in the Supplement). In 3 individuals with COVID-19, MHC class I and MHC class II expression on myofibers showed unequivocal perifascicular staining patterns (eFigure 1 in the Supplement).

Five individuals in the COVID-19 cohort (12%) showed marked infiltration by CD45-positive leukocytes and CD8-positive T cells (score >4 of 6). For all other biopsy samples, infiltrations of CD45-positive leukocytes and CD8-positive T cells were moderate to mild but significantly higher than in control samples (CD45: median [IQR], 28 [20] vs 13 [11] cells per 10 high-power fields; 95% CI, 7-33 cells per 10 high-power fields; $P < .001$; CD8: median [IQR], 7.5 [6.5] vs 2 [2]

Figure 3. Immunohistochemistry Showing Natural Killer Cells and No SARS-CoV-2 Spike Protein Detection

cells per 10 high-power fields; 95% CI, 1-9 cells per 10 high-power fields; $P < .001$; Figure 1 and 2; eTable 2 and eFigure 2 in the [Supplement](#)). We found NKp46-positive and CD56-positive natural killer cells in close contact with myofibers, and their numbers were increased compared with control samples (median [IQR], 8 [8] vs 3 [4] cells per 10 high-power fields; 95% CI, 1-10 cells per 10 high-power fields; $P < .001$; **Figure 3**; eTable 2 and eFigure 2 in the [Supplement](#)).

In 8 of 43 specimens (18%), we found notable capillary expression of human myxovirus resistance protein 1 (MxA). This finding was not present in control samples (**Figure 4**; eTable 2 in the [Supplement](#)).

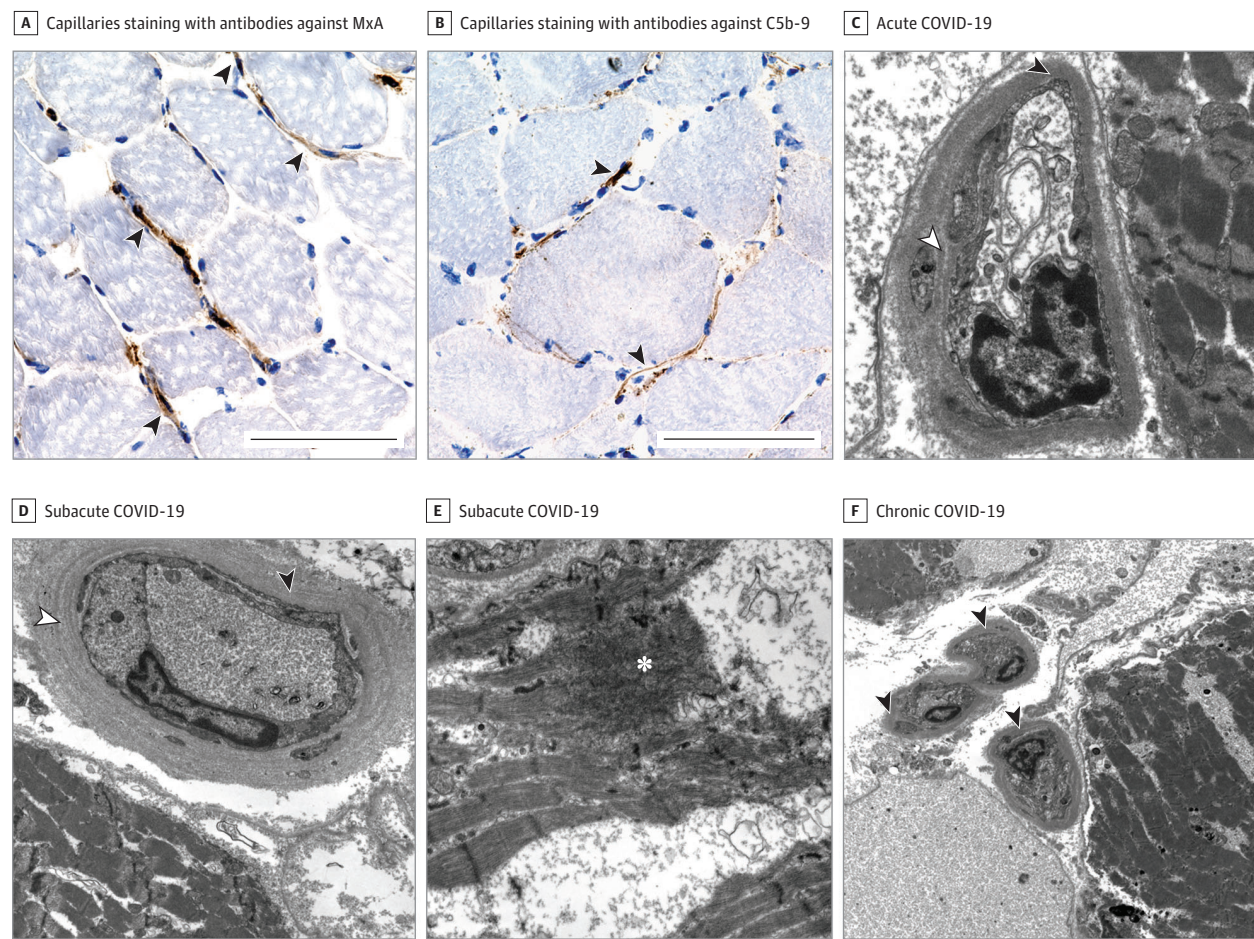
A subset of COVID-19 samples displayed signs of small and medium vessel angiitis, with perivascular infiltrates of

CD45-positive leukocytes, CD8-positive T cells, and CD68-positive macrophages but without transmural vessel infiltration (eFigure 1 in the [Supplement](#)). Necrotic fibers and capillary expression of C5b-9 were similarly found in specimens from patients with and without COVID-19. Of note, immunohistochemistry testing against SARS-CoV-2 spike protein did not yield positive results in skeletal muscle specimens that were positive by RT-qPCR (**Figure 3G**).

Histology and Immunohistochemistry of Heart Muscles

Numbers of myocardial CD68-positive macrophages were higher in patients with COVID-19 than control patients (median [IQR], 12 [25] vs 7 [10] macrophages; 95% CI, 1-20 macrophages; $P = .02$). Numbers of CD45-positive leukocytes

Figure 4. Immunohistochemical and Ultrastructural Analysis of Capillary Pathology



Representative light microscopic (A and B) and transmission electron microscopy images (C-F) of quadriceps specimens from patients who died with COVID-19. A, Capillary staining with antibodies against human myxovirus resistance protein 1 in a patient with an acute case (the patient coded as COVID29). B, Capillary staining with antibodies against C5b-9 in a patient with a subacute case (COVID05); original magnification, $\times 400$; scale bar: 100 μm . C-F, Ultrastructural analyses showing basement membrane thickening (C-D and F;

black arrowheads), basement membrane duplications (C-D; white arrowheads), sometimes by several layers (D, asterisks), and cytoplasmic bodies (E, asterisk). C, Image from a patient with an acute case (COVID07); original magnification: $\times 12\,000$. D, Image from a patient with a subacute case (COVID25); original magnification $\times 7000$. E, Image from a patient with a subacute case (COVID38), original magnification $\times 12\,000$. F, Image from a patient with a chronic case (COVID14); original magnification $\times 3000$.

and CD8-positive T cells were not significantly increased (Figure 1; eTable 2 in the Supplement). Numbers of myocardial CD45-positive leukocytes moderately correlated with numbers of CD45-positive leukocytes in skeletal muscle (Spearman r , 0.66; Pearson r , 0.71; $P < .001$; eFigure 3 in the Supplement). Immunohistochemistry against SARS-CoV-2 spike protein did not yield positive results in cardiac muscle specimens that were positive by RT-qPCR (Figure 3F).

Ultrastructural Analysis

Tubuloreticular inclusions as evidence of endothelial damage mediated by type I interferon were not found in any of the 5 analyzed samples with light microscopic signs of myositis. However, capillaries showed basement membrane thickening and duplications, sometimes by several layers. Pericyte processes were prominent around some capillaries and debris with whorled figures was found in others, indi-

cating a regenerative process after a primary injury. Endothelial cells were markedly thicker in many cases and harbored increased numbers of organelles with frequent swollen mitochondria and a granular appearance of cytoplasm with numerous ribosomes, indicating ongoing regenerative processes. Obstruction or acute thrombosis of small vessels was not observed. At many occasions, prominent cytoplasmic bodies as nonspecific indicators of severe muscle injury were identified (Figure 4).

Autoantibodies

In 10 patients with COVID-19, antinuclear antibody assays were performed during their lives, 2 of which showed a positive titer of 1:320. For 7 patients with COVID-19 and manifest myositis, serum samples were available for autoantibody profiling. None of the patients had relevant titers

of myositis-specific autoantibodies, but in samples from 1 young woman, Ro52 autoantibodies were present at low levels (eTable 3 in the [Supplement](#)).

Discussion

In this case-control study of patients who died with and without COVID-19, we found that most patients who died with severe COVID-19 displayed signs of myositis on a spectrum ranging from mild to severe inflammation. Significant upregulation of MHC class I antigens in the early phase of the disease and concomitant upregulation of MHC class II antigens on myofibers in later stages indicate involvement of skeletal muscle in the immune response against SARS-CoV-2. Inflammation of skeletal muscle correlated with DOI and inflammation of heart muscle. Overall, inflammatory changes were more pronounced in skeletal muscles than cardiac muscle, which is in line with findings suggesting myocarditis only in a subset of patients.⁴⁷⁻⁴⁹ In our study, some patients showed capillary expression of MxA, indicating a type I interferon signature and a perifascicular expression of MHC antigens, reminiscent of dermatomyositis.⁵⁰⁻⁵² However, we did not find MxA expression on the sarcolemma in any case, nor did we find tubuloreticular inclusions in capillaries of 5 selected patients, including 1 with capillary MxA expression and 2 with perifascicular MHC expression. Ultrastructural analysis revealed capillary alterations, suggesting ongoing remodeling processes. An important role for the vasculature niche has been described early in the pandemic.⁵³⁻⁵⁵

We identified natural killer cells in proximity to myofibers in many specimens and hypothesize that they may play a role in the pathogenesis of COVID-19-associated myositis. Natural killer cells are known first-line effector and regulator cells in viral disease, and their role in other types of myositis has been described.⁵⁶

In an autopsy case series from the 2003 outbreak of SARS-CoV-1, the authors found necrotic myofibers in 4 of 8 patients.⁵⁷ We found that necrotic myofibers and capillary complement deposition were not confined to muscles of patients with COVID-19. Therefore, we conclude that those findings are not specific but rather consequences of sepsis and/or critical illness.⁵⁸ With the heterogeneous course of COVID-19, with sometimes long stays in intensive care and often septic states, appropriate control groups are mandatory.⁵⁹ Our control group was comparable with the COVID-19 cohort with regard to invasive treatments, clinical and laboratory indicators of sepsis, and general systemic inflammation. Length of hospitalization and intensive care unit stays were longer in the cohort with COVID-19, as seen elsewhere.⁶⁰

Immunohistochemical staining with antibodies against SARS-CoV-2 spike protein did not yield positive results, and no overt viral particles were found by electron microscopy.⁶¹ Because increased blood levels of SARS-CoV-2 RNA were reported in patients with critical illness,⁶² it is conceivable that positivity by RT-qPCR is attributable to cir-

culating genomic viral RNA rather than genuine infection of myocytes. It has been shown that SARS-CoV-2 uses angiotensin-converting enzyme 2 (ACE2) in conjunction with transmembrane serine protease 2 and/or cathepsin L to enter host cells,^{63,64} and ACE2 seems to be expressed in human cardiomyocytes but not skeletal muscle.⁶⁵ A recent study did not find ACE2-transmembrane serine protease 2 and ACE2-cathepsin L coexpression in skeletal muscle tissue.⁶⁶ This, together with our findings that show significant inflammation mostly in individuals with subacute and chronic courses after seroconversion, argues for an immune-mediated myositis rather than a direct viral infection of myofibers.

Our study included patients from the first pandemic wave who did not receive corticosteroids. Interestingly, when compared with individuals affected more recently, who were treated with corticosteroids, we did not find a significant reduction of inflammation but found higher viral loads in respiratory tissues, which to our knowledge had not been described before now (eFigure 3 in the [Supplement](#)).

In 7 patients who died with COVID-19 and clear signs of myositis, we could obtain cryopreserved serum samples and performed autoimmune diagnostic tests by analyzing known myositis-specific and myositis-associated autoantibodies. One sample showed weakly positive results for anti-Ro52 testing, which has been associated with different types of myositis.⁶⁷⁻⁶⁹ Two of 10 patients with COVID-19 for whom an antinuclear antibody assay was performed during their lives showed a positive result, which is in line with other findings.⁷⁰⁻⁷²

Limitations

Morphological autopsy studies may be biased by autolytic changes. We used controls with comparable postmortem intervals to circumvent this.

Our cohort of patients with COVID-19 included only those with severe disease courses with fatal outcomes, which limits extrapolation to patients with mild SARS-CoV-2 infections. In addition, data on clinical correlates (myalgia, weakness) prior to death were scarce.

We included control specimens from patients with critical illness admitted to our intensive care unit who were SARS-CoV-2 negative and did not show clinical features of COVID-19. However, because this control cohort did not show evidence for other viral infections (eg, influenza), we cannot exclude that the findings in the COVID-19 cohort reflect general features of severe viral infection rather than effects specific to SARS-CoV-2 alone.

Because of the longer duration of intensive care treatment of the COVID-19 cohort compared with the control group, we cannot exclude that critical illness myopathy and intensive care unit-acquired weakness affected the morphology of skeletal muscle more in these patients than controls. However, the signs of myositis we observed are not typical features of critical illness myopathy.⁷³⁻⁷⁶

The same holds true for iatrogenic effects of myotoxic drugs. Prolonged treatment with corticosteroids may cause myopathic changes, and propofol has been associated with necrotizing myopathy but not with myositis.⁷⁷⁻⁸⁰

Conclusions

In this case-control study of patients who had died with and without COVID-19, most individuals with severe COVID-19 showed signs of myositis ranging from mild to severe.

SARS-CoV-2 may be associated with a postinfectious myositis in patients with severe illness. Whether these findings can be extrapolated to milder disease courses and potentially explain chronic muscle fatigue syndromes as described in post-acute COVID-19 syndromes and whether autoimmune mechanisms are involved will need to be addressed in future studies.

ARTICLE INFORMATION

Accepted for Publication: May 9, 2021.

Published Online: June 11, 2021.
doi:10.1001/jamaneurol.2021.2004

Correction: This article was corrected on August 12, 2021, to fix an error in Figure 1.

Author Affiliations: Department of Neuropathology, Charité-Universitätsmedizin Berlin, corporate member of Freie Universität Berlin and Humboldt-Universität zu Berlin, Berlin, Germany (Aschman, Meinhardt, Streit, Goebel, Radke, Radbruch, Heppner, Stenzel); Department of Virology, Charité-Universitätsmedizin Berlin, corporate member of Freie Universität Berlin and Humboldt-Universität zu Berlin, Berlin, Germany (Schneider, Drosten, Corman); Department of Pathology, Charité-Universitätsmedizin Berlin, corporate member of Freie Universität Berlin and Humboldt-Universität zu Berlin, Berlin, Germany (Greuel, Elez Kurtaj); Department of Autoimmune Diagnostics, Labor Berlin-Charité Vivantes GmbH, Berlin, Germany (Büttnerova); Department of Neurology and Experimental Neurology, Charité-Universitätsmedizin Berlin, corporate member of Freie Universität Berlin and Humboldt-Universität zu Berlin, Berlin, Germany (Scheibe); Institute for Medical Immunology, Charité-Universitätsmedizin Berlin, corporate member of Freie Universität Berlin and Humboldt-Universität zu Berlin, Berlin, Germany (Meisel); Berlin Institute of Health, Berlin, Germany (Heppner); Cluster of Excellence, NeuroCure, Berlin, Germany (Heppner); German Center for Neurodegenerative Diseases Berlin, Berlin, Germany (Heppner); Leibniz ScienceCampus Chronic Inflammation, Berlin, Germany (Stenzel).

Author Contributions: Drs Stenzel and Aschman had full access to all of the data in the study and take responsibility for the integrity of the data and the accuracy of the data analysis.

Concept and design: Aschman, Heppner, Stenzel.

Acquisition, analysis, or interpretation of data:

Aschman, Schneider, Greuel, Meinhardt, Streit, Goebel, Büttnerova, Elez Kurtaj, Scheibe, Radke, Meisel, Drosten, Radbruch, Corman, Stenzel.

Drafting of the manuscript: Aschman, Stenzel.

Critical revision of the manuscript for important intellectual content: Schneider, Greuel, Meinhardt, Streit, Goebel, Büttnerova, Elez Kurtaj, Scheibe, Radke, Drosten, Radbruch, Heppner, Corman, Stenzel.

Statistical analysis: Aschman.

Obtained funding: Drosten, Corman.

Administrative, technical, or material support:

Schneider, Greuel, Meinhardt, Streit, Büttnerova, Elez Kurtaj, Scheibe, Radke, Drosten, Radbruch, Heppner, Corman, Meisel, Stenzel.

Supervision: Goebel, Radke, Heppner, Corman, Stenzel.

Conflict of Interest Disclosures: Dr Corman reported grants from the German Ministry of Health, German Federal Ministry of Education and Research, and European Union's Horizon 2020

research during the conduct of the study; in addition, Dr Corman is named together with Euroimmun on a patent application filed recently regarding the diagnostic of SARS-CoV-2 by antibody testing. Dr Drosten reported grants from Horizon 2020 (RECOVER; grant GA101003589), the German Ministry of Health, and the German Federal Ministry of Education and Research (NaFoUniMedCovid19-PROVID, grant FKZ:01KX2021) during the conduct of the study. Dr Radbruch reported grants from the German Research Foundation (grant CRC 130 TP17) and the German Federal Ministry of Education and Research (Organostrat/Defeat Pandemics Netzwerk Universitätsmedizin) during the conduct of the study; and grants from Sanofi Foundation and Novartis Foundation and personal fees from Novartis and Sanofi outside the submitted work. Dr Heppner reported grants from the German Federal Ministry of Education and Research during the conduct of the study. No other disclosures were reported.

Funding/Support: The virological part of this work was funded by European Union's Horizon 2020 research and innovation program through RECOVER (grant GA101003589 [Dr Drosten]), the German Ministry of Health (Konsiliarlabor für Coronaviren and SeCoV [Drs Drosten and Corman]), and the German Federal Ministry of Education and Research (NaFoUniMedCovid19-PROVID; grant FKZ:01KX2021 [Drs Drosten and Corman]) and project VARIPath (grant OIKI2021 [Dr Corman]).

Role of the Funder/Sponsor: The funders had no role in the design and conduct of the study; collection, management, analysis, and interpretation of the data; preparation, review, or approval of the manuscript; and decision to submit the manuscript for publication.

Additional Contributions: We thank Francisca Egelhofer, Petra Matylewski, Cordula zum Bruch, Silvia Stefaniak, Department of Neuropathology, Charité-Universitätsmedizin, and Anistan Sebastianpillai, Department of Pathology, Charité Universitätsmedizin, for their excellent technical assistance. They were not compensated for their contributions.

REFERENCES

- Dong E, Du H, Gardner L. An interactive web-based dashboard to track COVID-19 in real time. *Lancet Infect Dis*. 2020;20(5):533-534. doi:10.1016/S1473-3099(20)30120-1
- Lechien JR, Chiesa-Estomba CM, Place S, et al; COVID-19 Task Force of YO-IFOS. Clinical and epidemiological characteristics of 1420 European patients with mild-to-moderate coronavirus disease 2019. *J Intern Med*. 2020;288(3):335-344. doi:10.1111/joim.13089
- Lai X, Wang M, Qin C, et al. Coronavirus disease 2019 (COVID-2019) infection among health care workers and implications for prevention measures

in a tertiary hospital in Wuhan, China. *JAMA Netw Open*. 2020;3(5):e209666. doi:10.1001/jamanetworkopen.2020.9666

- Lapostolle F, Schneider E, Vianu I, et al. Clinical features of 1487 COVID-19 patients with outpatient management in the greater Paris: the COVID-call study. *Intern Emerg Med*. 2020;15(5):813-817. doi:10.1007/s11739-020-02379-z
- Huang C, Wang Y, Li X, et al. Clinical features of patients infected with 2019 novel coronavirus in Wuhan, China. *Lancet*. 2020;395(10223):497-506. doi:10.1016/S0140-6736(20)30183-5
- Wang D, Hu B, Hu C, et al. Clinical characteristics of 138 hospitalized patients with 2019 novel coronavirus-infected pneumonia in Wuhan, China. *JAMA*. 2020;323(11):1061-1069. doi:10.1001/jama.2020.1585
- Mao L, Jin H, Wang M, et al. Neurologic manifestations of hospitalized patients with coronavirus disease 2019 in Wuhan, China. *JAMA Neurol*. 2020;77(6):683-690. doi:10.1001/jamaneurol.2020.1127
- Zhou F, Yu T, Du R, et al. Clinical course and risk factors for mortality of adult inpatients with COVID-19 in Wuhan, China: a retrospective cohort study. *Lancet*. 2020;395(10229):1054-1062. doi:10.1016/S0140-6736(20)30566-3
- Anwar H, Al Lawati A. Adolescent COVID-19-associated fatal rhabdomyolysis. *J Prim Care Community Health*. 2020;11:2150132720985641. doi:10.1177/2150132720985641
- Zhang Q, Shan KS, Minalyan A, O'Sullivan C, Nace T. A rare presentation of coronavirus disease 2019 (COVID-19) induced viral myositis with subsequent rhabdomyolysis. *Cureus*. 2020;12(5):e8074. doi:10.7759/cureus.8074
- Taxbro K, Kahlow H, Wulcan H, Fornarve A. Rhabdomyolysis and acute kidney injury in severe COVID-19 infection. *BMJ Case Rep*. 2020;13(9):e237616. doi:10.1136/bcr-2020-237616
- Husain R, Corcuera-Solano I, Dayan E, Jacobi AH, Huang M. Rhabdomyolysis as a manifestation of a severe case of COVID-19: a case report. *Radiol Case Rep*. 2020;15(9):1633-1637. doi:10.1016/j.radcr.2020.07.003
- Singh B, Kaur P, Mechineni A, Maroules M. Rhabdomyolysis in COVID-19: report of four cases. *Cureus*. 2020;12(9):e10686. doi:10.7759/cureus.10686
- Gefen AM, Palumbo N, Nathan SK, Singer PS, Castellanos-Reyes LJ, Sethna CB. Pediatric COVID-19-associated rhabdomyolysis: a case report. *Pediatr Nephrol*. 2020;35(8):1517-1520. doi:10.1007/s00467-020-04617-0
- Beydon M, Chevalier K, Al Tabaa O, et al. Myositis as a manifestation of SARS-CoV-2. *Ann Rheum Dis*. 2020;annrheumdis-2020-217573. doi:10.1136/annrheumdis-2020-217573
- Mehan WA, Yoon BC, Lang M, Li MD, Rincon S, Buch K. Paraspinal myositis in patients with

- COVID-19 infection. *AJNR Am J Neuroradiol*. 2020; 41(10):1949-1952. doi:10.3174/ajnr.A6711
17. Shabbir A, Camm CF, Elkington A, et al. Myopericarditis and myositis in a patient with COVID-19: a case report. *Eur Heart J Case Rep*. 2020;4(6):1-6. doi:10.1093/ehjcr/ytaa370
18. Ramani SL, Samet J, Franz CK, et al. Musculoskeletal involvement of COVID-19: review of imaging. *Skeletal Radiol*. 2021. doi:10.1007/s00256-021-03734-7
19. Manzano GS, Woods JK, Amato AA. Covid-19-associated myopathy caused by type I interferonopathy. *N Engl J Med*. 2020;383(24):2389-2390. doi:10.1056/NEJMc2031085
20. Zhang H, Charmchi Z, Seidman RJ, Anziska Y, Velayudhan V, Perk J. COVID-19-associated myositis with severe proximal and bulbar weakness. *Muscle Nerve*. 2020;62(3):E57-E60. doi:10.1002/mus.27003
21. Tanboon J, Nishino I. COVID-19-associated myositis may be dermatomyositis. *Muscle Nerve*. 2021;63(1):E9-E10. doi:10.1002/mus.27105
22. Huang C, Huang L, Wang Y, et al. 6-month consequences of COVID-19 in patients discharged from hospital: a cohort study. *Lancet*. 2021;397(10270):220-232. doi:10.1016/S0140-6736(20)32656-8
23. Nalbandian A, Sehgal K, Gupta A, et al. Post-acute COVID-19 syndrome. *Nat Med*. 2021;27(4):601-615. doi:10.1038/s41591-021-01283-z
24. Moreno-Pérez O, Merino E, Leon-Ramírez JM, et al; COVID19-ALC research group. Post-acute COVID-19 syndrome: incidence and risk factors, a Mediterranean cohort study. *J Infect*. 2021;82(3):378-383. doi:10.1016/j.jinf.2021.01.004
25. Smith RD, Konoplev S, DeCourten-Myers G, Brown T. West Nile virus encephalitis with myositis and orchitis. *Hum Pathol*. 2004;35(2):254-258. doi:10.1016/j.humpath.2003.09.007
26. O'Connor JV, Iyer SK. Myoglobinuria associated with parainfluenza type 2 infection. *N Y State J Med*. 1982;82(10):1469-1470.
27. Wright J, Couchonnal G, Hodges GR. Adenovirus type 21 infection: occurrence with pneumonia, rhabdomyolysis, and myoglobinuria in an adult. *JAMA*. 1979;241(22):2420-2421. doi:10.1001/jama.1979.03290480054026
28. Seibold S, Merkel F, Weber M, Marx M. Rhabdomyolysis and acute renal failure in an adult with measles virus infection. *Nephrol Dial Transplant*. 1998;13(7):1829-1831. doi:10.1093/ndt/13.7.1829
29. Finsterer J, Kongchan K. Severe, persisting, steroid-responsive dengue myositis. *J Clin Virol*. 2006;35(4):426-428. doi:10.1016/j.jcv.2005.11.010
30. Mall S, Buchholz U, Tibussek D, et al. A large outbreak of influenza B-associated benign acute childhood myositis in Germany, 2007/2008. *Pediatr Infect Dis J*. 2011;30(8):e142-e146. doi:10.1097/INF.0b013e318217e356
31. Hu JJ, Kao CL, Lee PI, et al. Clinical features of influenza A and B in children and association with myositis. *J Microbiol Immunol Infect*. 2004;37(2):95-98.
32. Yoshino M, Suzuki S, Adachi K, Fukayama M, Inamatsu T. High incidence of acute myositis with type A influenza virus infection in the elderly. *Intern Med*. 2000;39(5):431-432. doi:10.2169/internalmedicine.39.431
33. Middleton PJ, Alexander RM, Szymanski MT. Severe myositis during recovery from influenza. *Lancet*. 1970;2(7672):533-535. doi:10.1016/S0140-6736(70)91343-7
34. Charriot P, Ruet E, Authier FJ, Lévy Y, Gherardi R. Acute rhabdomyolysis in patients infected by human immunodeficiency virus. *Neurology*. 1994; 44(9):1692-1696. doi:10.1212/WNL.44.9.1692
35. Hughes GS Jr, Hunt R. Cytomegalovirus infection with rhabdomyolysis and myoglobinuria. *Ann Intern Med*. 1984;101(2):276-277. doi:10.7326/0003-4819-101-2-276_2
36. McCabe JL, Duckett S, Kaplan P. Epstein-Barr virus infection complicated by acute rhabdomyolysis. *Am J Emerg Med*. 1988;6(5):453-455. doi:10.1016/0735-6757(88)90244-6
37. Fodili F, van Bommel EF. Severe rhabdomyolysis and acute renal failure following recent Coxsackie B virus infection. *Neth J Med*. 2003;61(5):177-179.
38. Jehn UW, Fink MK. Myositis, myoglobinemia, and myoglobinuria associated with enterovirus echo 9 infection. *Arch Neurol*. 1980;37(7):457-458. doi:10.1001/archneur.1980.00500560087016
39. Josselson J, Pula T, Sadler JH. Acute rhabdomyolysis associated with an echovirus 9 infection. *Arch Intern Med*. 1980;140(12):1671-1672. doi:10.1001/archinte.1980.0033023017025
40. Erhardt CL. What is the cause of death. *J Am Med Assoc*. 1958;168(2):161-168. doi:10.1001/jama.1958.030000200220005
41. Corman VM, Landt O, Kaiser M, et al. Detection of 2019 novel coronavirus (2019-nCoV) by real-time RT-PCR. *Euro Surveill*. 2020;25(3). doi:10.2807/1560-7917.ES.2020.25.3.2000045
42. Meinhardt J, Radke J, Dittmayer C, et al. Olfactory transmucosal SARS-CoV-2 invasion as a port of central nervous system entry in individuals with COVID-19. *Nat Neurosci*. 2021;24(2):168-175. doi:10.1038/s41593-020-00758-5
43. Wölfel R, Corman VM, Guggemos W, et al. Virological assessment of hospitalized patients with COVID-2019. *Nature*. 2020;581(7809):465-469. doi:10.1038/s41586-020-2196-x
44. Preuß C, Allenbach Y, Hoffmann O, et al. Differential roles of hypoxia and innate immunity in juvenile and adult dermatomyositis. *Acta Neuropathol Commun*. 2016;4(1):45. doi:10.1186/s40478-016-0308-5
45. Wedderburn LR, Varsani H, Li CK, et al; UK Juvenile Dermatomyositis Research Group. International consensus on a proposed score system for muscle biopsy evaluation in patients with juvenile dermatomyositis: a tool for potential use in clinical trials. *Arthritis Rheum*. 2007;57(7):1192-1201. doi:10.1002/art.23012
46. Demsar J, Curk T, Erjavec A, et al Orange: Data Mining Toolbox in Python. *J Mach Learn Res*. Aug 2013;14:2349-2353.
47. Lindner D, Fitzek A, Bräuninger H, et al. Association of cardiac infection with SARS-CoV-2 in confirmed COVID-19 autopsy cases. *JAMA Cardiol*. 2020;5(11):1281-1285. doi:10.1001/jamacardio.2020.3551
48. Roshdy A, Zaher S, Fayed H, Coghlan JG. COVID-19 and the heart: a systematic review of cardiac autopsies. *Front Cardiovasc Med*. 2021;7:626975. doi:10.3389/fcvm.2020.626975
49. Halushka MK, Vander Heide RS. Myocarditis is rare in COVID-19 autopsies: cardiovascular findings across 277 postmortem examinations. *Cardiovasc Pathol*. 2021;50:107300. doi:10.1016/j.carpath.2020.107300
50. Mammen AL, Allenbach Y, Stenzel W, Benveniste O; ENMC 239th Workshop Study Group. 239th ENMC International Workshop: classification of dermatomyositis, Amsterdam, the Netherlands, 14-16 December 2018. *Neuromuscul Disord*. 2020; 30(1):70-92. doi:10.1016/j.nmd.2019.10.005
51. Uruha A, Nishikawa A, Tsuburaya RS, et al. Sarcoplasmic MxA expression: a valuable marker of dermatomyositis. *Neurology*. 2017;88(5):493-500. doi:10.1212/WNL.0000000000003568
52. Benveniste O, Goebel HH, Stenzel W. Biomarkers in inflammatory myopathies—an expanded definition. *Front Neurol*. 2019;10:554. doi:10.3389/fneur.2019.00554
53. Ackermann M, Verleden SE, Kuehnel M, et al. Pulmonary vascular endothelialitis, thrombosis, and angiogenesis in Covid-19. *N Engl J Med*. 2020;383(2):120-128. doi:10.1056/NEJMoa2015432
54. Varga Z, Flammer AJ, Steiger P, et al. Endothelial cell infection and endothelitis in COVID-19. *Lancet*. 2020;395(10234):1417-1418. doi:10.1016/S0140-6736(20)30937-5
55. Teuwen LA, Geldhof V, Pasut A, Carmeliet P. COVID-19: the vasculature unleashed. *Nat Rev Immunol*. 2020;20(7):389-391. doi:10.1038/s41577-020-0343-0
56. Hervier B, Perez M, Allenbach Y, et al. Involvement of NK cells and Nkp30 pathway in antisynthetase syndrome. *J Immunol*. 2016;197(5):1621-1630. doi:10.4049/jimmunol.1501902
57. Leung TW, Wong KS, Hui AC, et al. Myopathic changes associated with severe acute respiratory syndrome: a postmortem case series. *Arch Neurol*. 2005;62(7):1113-1117. doi:10.1001/archneur.62.7.1113
58. Charchafieh J, Wei J, Labaze G, et al. The role of complement system in septic shock. *Clin Dev Immunol*. 2012;2012:407324. doi:10.1155/2012/407324
59. Deigendesch N, Sironi L, Kutza M, et al. Correlates of critical illness-related encephalopathy predominate postmortem COVID-19 neuropathology. *Acta Neuropathol*. 2020;140(4):583-586. doi:10.1007/s00401-020-02213-y
60. Socolovitch RL, Fumis RRL, Tomazini BM, et al. Epidemiology, outcomes, and the use of intensive care unit resources of critically ill patients diagnosed with COVID-19 in Sao Paulo, Brazil: a cohort study. *PLoS One*. 2020;15(12):e0243269. doi:10.1371/journal.pone.0243269
61. Dittmayer C, Meinhardt J, Radbruch H, et al. Why misinterpretation of electron micrographs in SARS-CoV-2-infected tissue goes viral. *Lancet*. 2020;396(10260):e64-e65. doi:10.1016/S0140-6736(20)32079-1
62. Buetti N, Patrier J, Le Hingrat Q, et al. Risk factors for severe acute respiratory syndrome coronavirus 2 (SARS-CoV-2) detection in blood of critically ill patients. *clin infect dis*. 2021;72(10):e690-e691.
63. Walls AC, Park YJ, Tortorici MA, Wall A, McGuire AT, Veeseleer D. Structure, function, and antigenicity of the SARS-CoV-2 spike glycoprotein. *Cell*. 2020; 183(6):1735. doi:10.1016/j.cell.2020.11.032

64. Hoffmann M, Kleine-Weber H, Schroeder S, et al. SARS-CoV-2 cell entry depends on ACE2 and TMPRSS2 and is blocked by a clinically proven protease inhibitor. *Cell*. 2020;181(2):271-280.e8. doi:10.1016/j.cell.2020.02.052
65. Hikmet F, Méar L, Edvinsson Å, Micke P, Uhlén M, Lindskog C. The protein expression profile of ACE2 in human tissues. *Mol Syst Biol*. 2020;16(7):e9610. doi:10.15252/msb.20209610
66. Muus C, Luecken MD, Eraslan G, et al; NHLBI LungMap Consortium; Human Cell Atlas Lung Biological Network. Single-cell meta-analysis of SARS-CoV-2 entry genes across tissues and demographics. *Nat Med*. 2021;27(3):546-559. doi:10.1038/s41591-020-01227-z
67. Sabbagh S, Pinal-Fernandez I, Kishi T, et al; Childhood Myositis Heterogeneity Collaborative Study Group. Anti-Ro52 autoantibodies are associated with interstitial lung disease and more severe disease in patients with juvenile myositis. *Ann Rheum Dis*. 2019;78(7):988-995. doi:10.1136/annrheumdis-2018-215004
68. Frank MB, McCubbin V, Trieu E, Wu Y, Isenberg DA, Targoff IN. The association of anti-Ro52 autoantibodies with myositis and scleroderma autoantibodies. *J Autoimmun*. 1999;12(2):137-142. doi:10.1006/jaut.1998.0265
69. Temmoku J, Sato S, Fujita Y, et al. Clinical significance of myositis-specific autoantibody profiles in Japanese patients with polymyositis/dermatomyositis. *Medicine (Baltimore)*. 2019;98(20):e15578. doi:10.1097/MD.00000000000015578
70. Chang SE, Feng A, Meng W, et al New-onset IgG autoantibodies in hospitalized patients with COVID-19. *medRxiv*. Jan 29 2021;doi:10.1101/2021.01.27.21250559
71. Vlachoyiannopoulos PG, Magira E, Alexopoulos H, et al. Autoantibodies related to systemic autoimmune rheumatic diseases in severely ill patients with COVID-19. *Ann Rheum Dis*. 2020;79(12):1661-1663. doi:10.1136/annrheumdis-2020-218009
72. Wang EY, Mao T, Klein J, et al Diverse functional autoantibodies in patients with COVID-19. *medRxiv*. Dec 12 2020;doi:10.1101/2020.12.10.20247205
73. Zink W, Kollmar R, Schwab S. Critical illness polyneuropathy and myopathy in the intensive care unit. *Nat Rev Neurol*. 2009;5(7):372-379. doi:10.1038/nrneurol.2009.75
74. Hund E. Myopathy in critically ill patients. *Crit Care Med*. 1999;27(11):2544-2547. doi:10.1097/00003246-199911000-00036
75. Helliwell TR, Coakley JH, Wagenmakers AJ, et al. Necrotizing myopathy in critically-ill patients. *J Pathol*. 1991;164(4):307-314. doi:10.1002/path.1711640406
76. Derde S, Hermans G, Derese I, et al. Muscle atrophy and preferential loss of myosin in prolonged critically ill patients. *Crit Care Med*. 2012;40(1):79-89. doi:10.1097/CCM.0b013e31822d7c18
77. Khaleeli AA, Edwards RH, Gohil K, et al. Corticosteroid myopathy: a clinical and pathological study. *Clin Endocrinol (Oxf)*. 1983;18(2):155-166. doi:10.1111/j.1365-2265.1983.tb03198.x
78. Braunstein PW Jr, DeGirolami U. Experimental corticosteroid myopathy. *Acta Neuropathol*. 1981;55(3):167-172. doi:10.1007/BF00691314
79. Afifi AK, Bergman RA, Harvey JC. Steroid myopathy: clinical, histologic and cytologic observations. *Johns Hopkins Med J*. 1968;123(4):158-173.
80. Doughty CT, Amato AA. Toxic myopathies. *Continuum (Minneap Minn)*. 2019;25(6):1712-1731. doi:10.1212/CON.0000000000000806